(Received 30 November 2023, Accepted 27 December 2023, Scheduled 9 January 2024)

A High Efficiency and Low Mutual Coupling Four-Element Antenna Array for GNSS Applications

Abdullah Madni[1,*] and Wasif Tanveer Khan[1,2]

[1] Lahore University of Management Sciences (LUMS), Lahore, Pakistan
[2] National University of Sciences and Technology (NUST), Islamabad, Pakistan

ABSTRACT: In this manuscript, a compact four-element antenna array is introduced for global navigation satellite system (GNSS) upper L-band applications. The proposed design is modelled using a higher epsilon substrate to obtain a smaller patch footprint. The array consists of four rectangular right-hand circularly polarized (RHCP) patches etched on a circular substrate having a compact diameter of only 125 mm. The patch elements cover the BeiDou B1 (1561.098 MHz), GPS L1 (1575.42 MHz), Galileo E1 (1575.42 MHz), and GLONASS G1 (1602 MHz) bands with an axial ratio below 3 dB. A defected ground structure (DGS) has been integrated in the ground plane of the proposed array along with a novel meta-isolator on the top side between the antennas to achieve a high isolation level of more than 24 dB in the complete band of interest. The proposed antenna array has a high gain of more than 6.9 dBi and a radiation efficiency greater than 93%. A prototype of the proposed array is fabricated, and measured results are presented to validate the design.

1. INTRODUCTION

Recently global navigation satellite systems (GNSSs) like GPS, BeiDou, Galileo, and GLONASS have advanced substantially. These services are divided into different sub-bands such as lower L-band (1.151–1.214 GHz) and upper L-band (1.559–1.610 GHz) [1]. In this work, we will be focusing on designing a four element antenna array for the upper L-band that consists of BeiDou B1 band (1561.098 MHz), GPS L1 band (1575.42 MHz), Galileo E1 band (1575.42 MHz), and GLONASS G1 band (1602 MHz).

GNSSs use antenna arrays having multiple elements to achieve high gain and anti-jamming capability by creating nulls and steering them in the direction of potential jammers. In addition to high gain and anti-jamming, it is also prudent to have antenna arrays with high inter-element isolation. High mutual coupling between the antenna elements causes radiation pattern distortion [2]. Furthermore, in GNSS arrays mutual coupling is highly inadmissible since it degenerates nulling depth and radiation efficiency [3]. Hence, the main challenge in designing GNSS arrays is to mitigate the mutual coupling within a compact size.

Various methods have been proposed to mitigate mutual coupling in compact antenna arrays such as in [4]. Electromagnetic Band Gap (EBG) surface is proposed to suppress the coupling to -24 dB. However, EBGs give narrowband isolation levels and are complex to fabricate due to the presence of vias. Metamaterials such as split ring resonators (SSRs) have also been used to mitigate the mutual coupling in GNSS arrays [5]. However, they are polarization dependent, and their isolating capability depends on their position with reference to the magnetic field component [6].

Recently, microwave absorber materials have also been utilized to enhance the isolation level in GNSS arrays as in [7], and a 9.525 mm high MT-30 material is employed to enhance the isolation level above 20 dB. In [8], a 3.175 mm MT-30 material has been used in combination with a DGS for isolation enhancement to up to 25 dB. However, the gains of these reported designs are only greater than 3.3 dBi and 5.75 dBi, respectively. Meanwhile, the corresponding radiation efficiencies are only above 38% and 58.8%, respectively. GNSS antennas must exhibit adequate gain to compensate the inherently weak signals transmitted by GNSS satellites, particularly in the presence of atmospheric attenuation and adverse weather conditions. Low-gain and low efficiency antennas can lead to signal degradation and impact the ability to accurately track GNSS satellites [9, 10]. Hence, it is important to achieve a balance between isolation enhancement and maintaining sufficient gain and efficiency in such designs for robust performance. Some other GNSS designs have been reported in [14–18], but they suffer from large dimensions, fewer GNSS bands covered, less isolation level, less gain and design complexity compared to our presented design.

In this work, the problem of lower gain and radiation efficiency is resolved by proposing a four-element DGS-based antenna array consisting of a novel meta-isolator that is placed between the radiating patches. The presented antenna provides a complete band coverage across all GNSS services of the upper L-band. An isolation above 24 dB is attained in the complete band of interest without compromising the radiation efficiency and gain of the proposed array.

* Corresponding author: Abdullah Madni (19060037@lums.edu.pk).

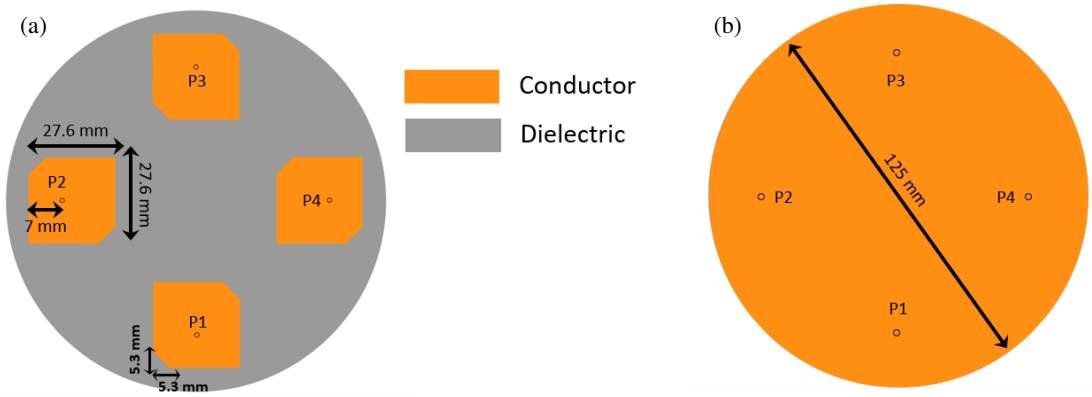

FIGURE 1. Design configuration of the proposed array with no decoupling mechanism. (a) Top surface. (b) Bottom surface.

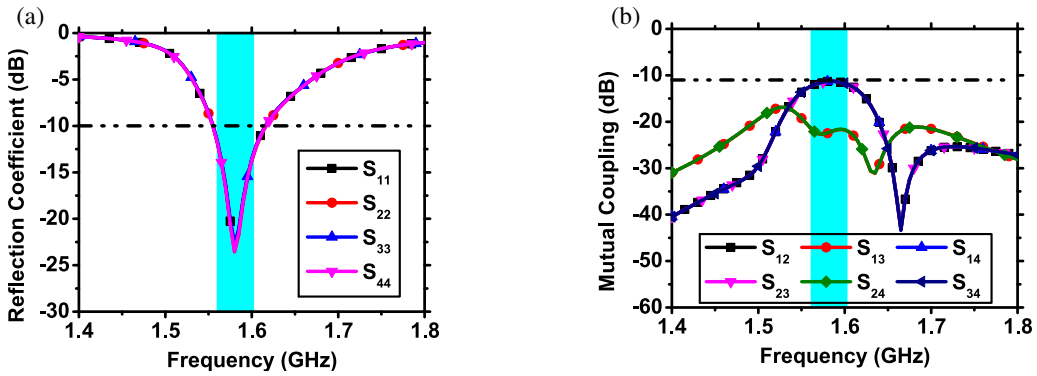

FIGURE 2. Simulation results of the presented design with no decoupling mechanism. (a) Impedance matching response. (b) Mutual coupling response.

2. ARRAY WITH NO DECOUPLING STRUCTURE

In the first stage, an array without any decoupling structure was modelled. The array comprises four identical square patches etched on a 125 mm diameter and 5.08 mm thick Rogers TMM10i ($\epsilon_r = 10.2$, $\tan\delta = 0.002$) substrate featuring a full ground plane. The four radiating elements are positioned in a chronologically rotated configuration, and this layout has also been exploited to yield circular polarization (CP) from linearly polarized antennas [11]. Moreover, the rotational symmetry also helps in packing more antennas within a confined area. This design arrangement is also helpful in achieving better circular polarization (CP) and creating nulls for the anti-jamming capability [7]. The patches have their corners diagonally truncated to attain CP which is essential for GNSS antennas. The antenna is modelled using High Frequency Structure Simulator (HFSS) software. Each patch is fed by a 50-ohm coaxial port also modelled in HFSS. Each port comprises a feeding pin which is surrounded by teflon and an outer conductor that encapsulates the whole assembly. Owing to a symmetrically rotated configuration, the ports are given a phase shift of $P1 = 0°$, $P2 = 90°$, $P3 = 180°$, and $P4 = 270°$ [7]. Fig. 1 shows the design configuration of the proposed array.

The impedance matching response and mutual coupling of the proposed simple four element antenna array without any decoupling structure are simulated. The bandwidth being occupied is from 1.56 to 1.62 GHz. The mutual coupling can be split into two groups, i.e., coupling between the nearest neighboring antennas ($S_{12}, S_{14}, S_{23}, S_{34}$) and the coupling amid the opposite elements (S_{13}, S_{24}). The coupling between the nearest neighboring elements is lower than only -11 dB owing to their closer vicinity whereas for the opposite elements, the coupling is below -20 dB. It can be noted that due to symmetrical design geometry, $S_{11} = S_{22} = S_{33} = S_{44}$ and $S_{12} = S_{21}$, $S_{13} = S_{31}$ and so on. The overall mutual coupling is only less than -11 dB. Fig. 2 illustrates the simulated results of the proposed four-element antenna array with no decoupling structure.

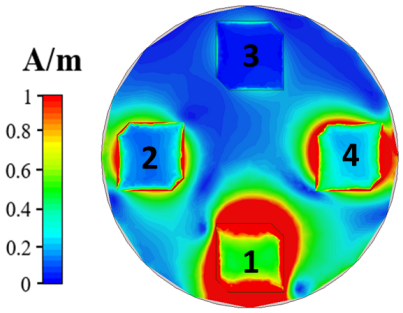

FIGURE 3. Simulated surface current distribution at 1.575 GHz with no decoupling mechanism.

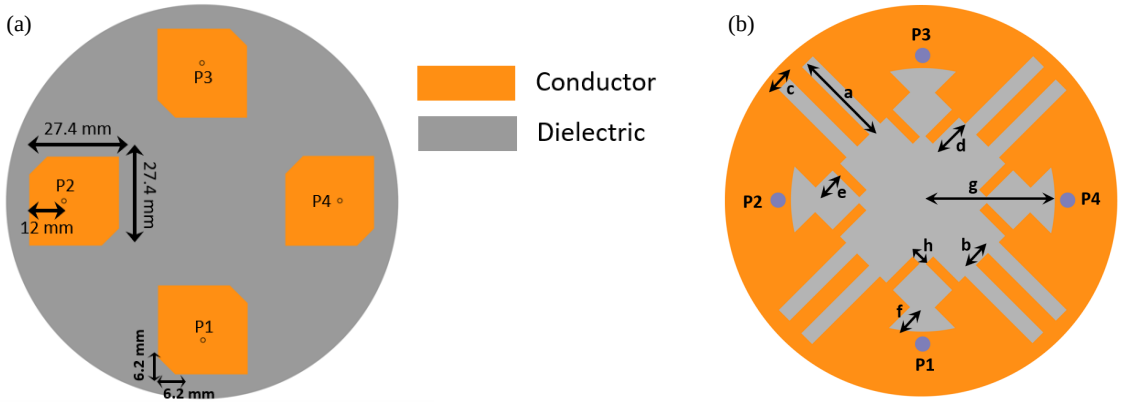

FIGURE 4. Design configuration of the presented array with DGS. (a) Top surface. (b) Bottom surface ($a = 30.25$ mm, $b = 8.7$ mm, $c = 1.75$ mm, $d = 11.75$ mm, $e = 8.47$ mm, $f = 9.02$ mm, $g = 42$ mm, $h = 3$ mm).

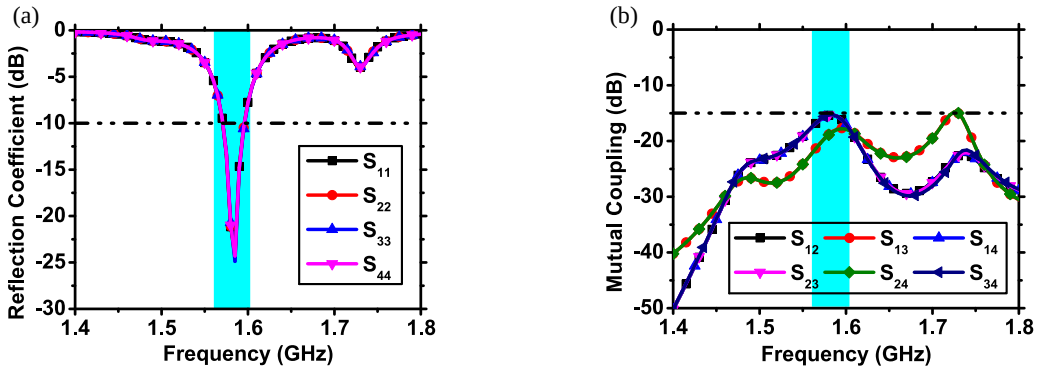

FIGURE 5. Simulation results of the proposed array with DGS only. (a) Impedance matching response. (b) Mutual coupling response.

The simulated surface current distribution of the design at 1.575 GHz (GPS L1 band) is shown in Fig. 3. It can be observed that strong coupling is present between the orthogonally placed elements like element 1 and element 2 due to a small distance between them. The linearly placed elements like element 1 and 3 are better isolated from each other due to a greater distance between them.

3. ARRAY WITH DEFECTED GROUND STRUCTURE (DGS)

The surface current distribution in Fig. 3 shows that strong coupling is present between the orthogonally placed elements. Therefore, a novel defected ground structure (DGS) with slots at the regions of higher coupling is employed in the ground plane of the proposed antenna to enhance the isolation level. When DGS is employed, the size of the patch elements, patch corner truncations, and distance from the feed is slightly changed to 27.4 mm, 6.2 mm, and 12 mm respectively to tune the array to resonate at 1.575 GHz for better impedance matching and optimum performance. Fig. 4 shows the four-element array with DGS.

The impedance matching response and mutual coupling of the proposed four element antenna array with DGS are simulated. It can be noticed that the mutual coupling is lower than -15.6 dB in the complete desired bandwidth. Therefore, an enhancement of 4.6 dB in the isolation level is attained after employing the presented DGS. Fig. 5 presents these results.

The impact of the DGS can be seen by simulating the surface current distribution at 1.575 GHz which shows the current being trapped by the DGS slots as observed in Fig. 6.

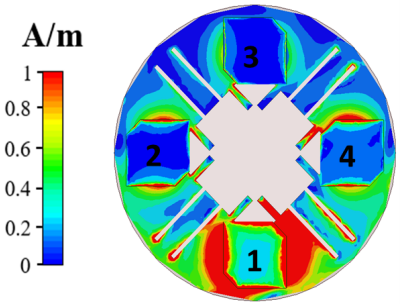

FIGURE 6. Simulated surface current distribution at 1.575 GHz with DGS.

4. ARRAY WITH DGS AND META-ISOLATOR

With the aim of further enhancing the isolation level, a novel meta-isolator is placed between the antenna patches on the top

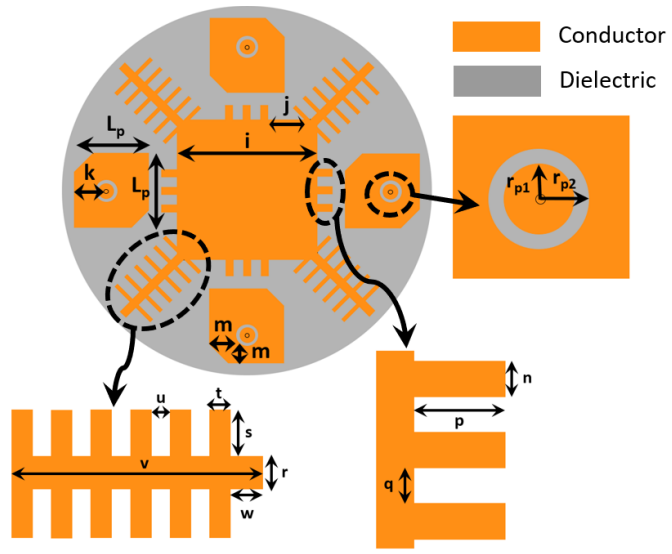

FIGURE 7. Design configuration of the four-element array with both DGS and meta-isolator ($i = 48\,\text{mm}$, $j = 11\,\text{mm}$, $k = 7\,\text{mm}$, $L_p = 25\,\text{mm}$, $m = 5.6\,\text{mm}$, $n = 2\,\text{mm}$, $p = 5\,\text{mm}$, $q = 4\,\text{mm}$, $r_{rp1} = 2.7\,\text{mm}$, $r_{rp2} = 3.1\,\text{mm}$, $r = 3\,\text{mm}$, $s = 7\,\text{mm}$, $t = 0.6\,\text{mm}$, $u = 4.4\,\text{mm}$, $v = 27.5\,\text{mm}$ and $w = 4.7\,\text{mm}$).

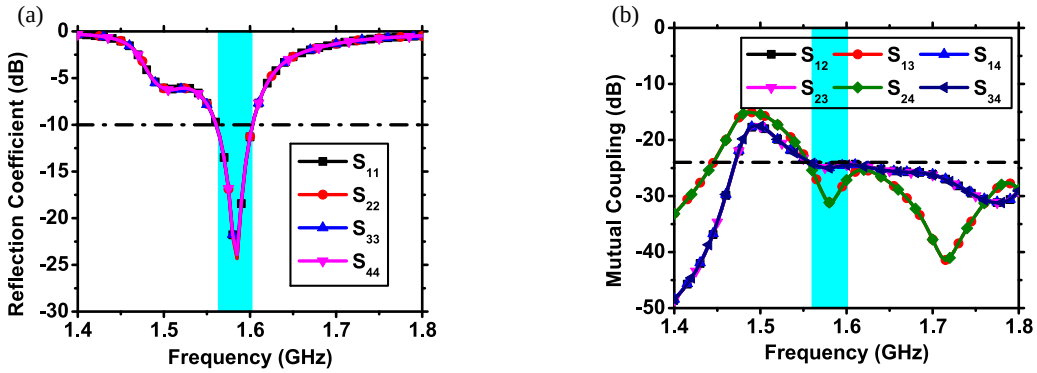

FIGURE 8. Simulation results of the presented design with DGS and meta-isolator. (a) Impedance matching response. (b) Mutual coupling.

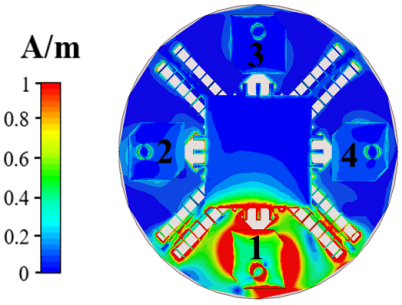

FIGURE 9. Simulated surface current distribution at 1.575 GHz with DGS and meta-isolator.

surface of the DGS based design as illustrated in Fig. 7. When the meta-isolator is placed between the radiating patches, the input impedance is altered resulting in a change in the impedance matching response. Hence, the sizes of the patch elements and the distance of the feed point from the edge of the patch have been re-optimized. Furthermore, an annular gap has also been added in each of the four patches to improve the reflection coefficient such that the required bandwidth of interest is occupied. This technique is useful for achieving wider bandwidth in thicker substrates [12]. In the ground plane of the antenna (Fig. 4(b)), we have chosen $d = 10\,\text{mm}$, $e = 9.83\,\text{mm}$, $f = 14.47\,\text{mm}$, $g = 46\,\text{mm}$, and $h = 4\,\text{mm}$ for optimum performance in the GNSS L1 band. Fig. 8 shows the simulated reflection coefficient and mutual coupling of the proposed configuration. It can be observed that that all the required GNSS bands of interest are covered with an isolation level above 24 dB. Therefore, there is an isolation improvement of 8.4 dB by using a meta-isolator along with a DGS as compared to using DGS only. The simulated surface current distribution of the proposed meta-isolator based design is exhibited in Fig. 9 showing that current propagation responsible for higher coupling is completely blocked. This indicates the effectiveness of our proposed DGS and meta-isolator that are responsible for improving the isolation level significantly.

The simulated 2D radiation pattern of the presented 4-element array at 1.575 GHz shows that the array has a gain of more than 6 dBi. The radiation pattern is almost hemispherical

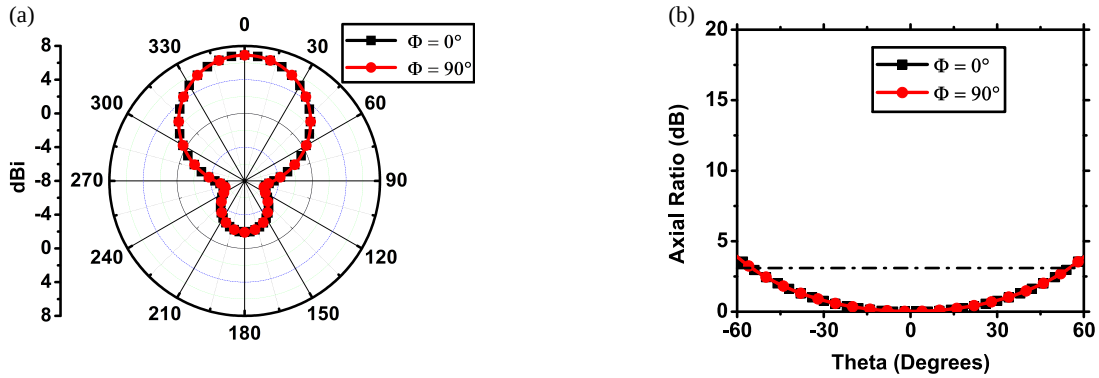

FIGURE 10. Simulation results of the presented array with DGS and meta-isolator. (a) 2D radiation pattern. (b) Axial ratio.

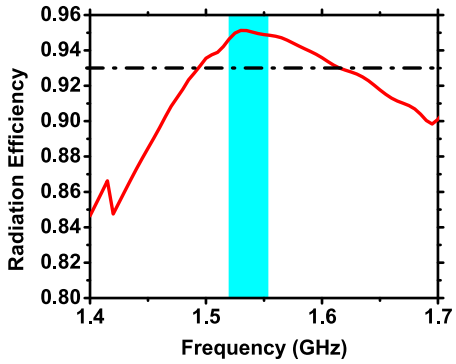

FIGURE 11. Simulated radiation efficiency of the presented DGS and meta-isolator array.

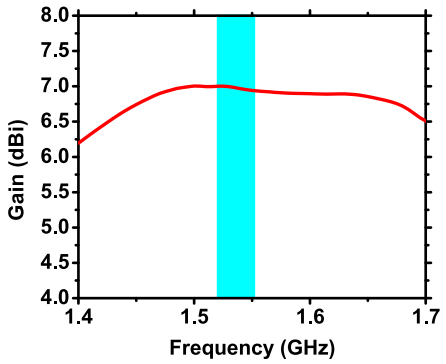

FIGURE 12. Simulated gain of the proposed DGS and meta-isolator array.

showing that the presented design is able to encompass the full upper half spherical beam facing the sky for robust performance. For good CP performance the axial ratio should be less than 3 dB [13]. The simulated axial ratio of our proposed antenna array is less than 3 dB with a beamwidth about 120°. Fig. 10 exhibits these results.

The radiation efficiency of the presented 4-element array with a DGS and meta-isolator is more than 93% in the entire BW of interest while the gain is more than 6.9 dBi with a peak value of 6.93i dB at 1.561 GHz as shown in Fig. 11 and Fig. 12, respectively.

The variation of RHCP and left-hand circularly polarized (LHCP) realized gains with polar angle and frequency are shown in Fig. 13 for 1.575 GHz (GPS L1 band).

It can be observed that the LHCP component is significantly less than the RHCP component indicating that the proposed antenna array has excellent polarization purity.

5. FABRICATION AND MEASURED RESULTS

The previous section shows that the DGS and meta-isolator design exhibits excellent characteristics in all aspects such as GNSS band coverage, isolation, and CP performance and is therefore our finalized model. It is fabricated by means of LPKF S103 rapid prototype milling machine using a Rogers TMM10i substrate (5.08 mm thick) as shown in Fig. 14. The S-parameters of the fabricated model were measured by employing a Rhode and Schwarz vector network analyzer (VNA) ZVA 40 as shown in Fig. 15.

The mutual coupling is lower than -24 dB while all the GNSS bands of interest are occupied. It can be observed that the maximum isolation at the GPS L1 band (1.575 GHz) is 30.4 dB while at the BeiDou B1 (1.561 GHz) and GLONASS G1 bands (1.602 GHz), the highest value of isolation is 26 dB and 32 dB, respectively. The radiation pattern of the proposed DGS and meta-isolator design was measured in an anechoic chamber using a 1–4 power divider as shown in Fig. 16.

In Fig. 17, the presented radiation pattern demonstrates the formation of a null directed towards boresight at 1.575 GHz. This pattern is achieved by concurrently exciting all four ports in the anechoic chamber, employing a 1–4 power splitter. The measured null depth exceeds 40 dB which is consistent with the simulation.

The normalized E and H-plane RHCP and LHCP radiation patterns are shown in Fig. 18 when only a single port is excited at 1.575 GHz. It can be seen that the presented antenna array has good polarization purity with a reduced LHCP component making it an ideal option for robust GNSS multi-band applications. Moreover, the RHCP pattern shows that the proposed antenna covers the upper hemisphere facing the sky ensuring good GNSS coverage for optimum performance.

Table 1 presents a comparative analysis between our proposed design and the existing designs reported earlier in the literature.

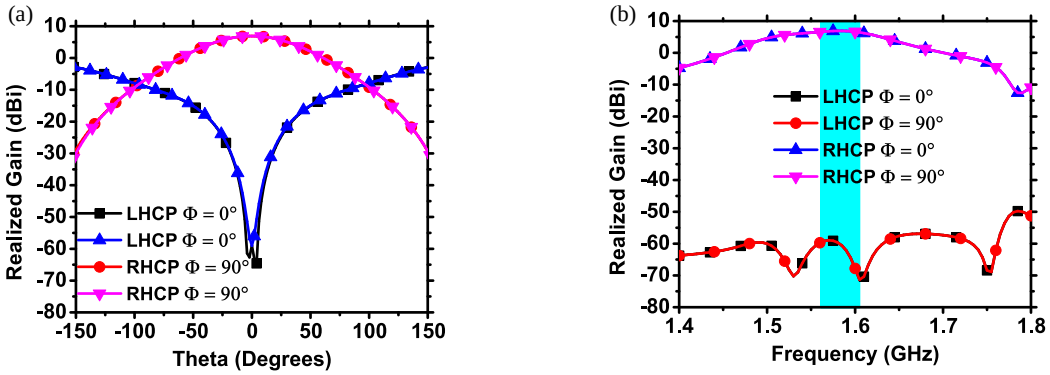

FIGURE 13. Simulation results of the proposed array with DGS and meta-isolator. (a) Realized CP gain variation with theta. (b) Realized CP gain variation with frequency.

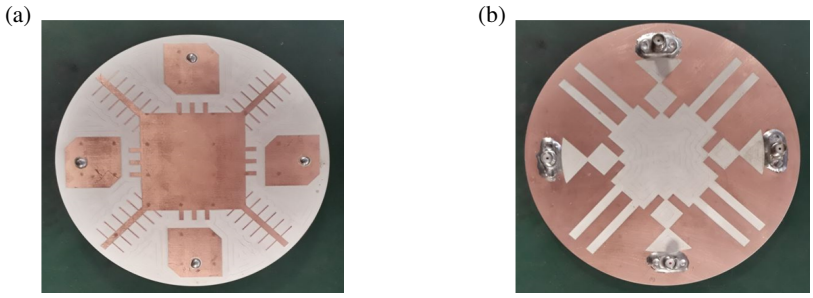

FIGURE 14. Fabricated DGS and meta-isolator array. (a) Top side. (b) Bottom side.

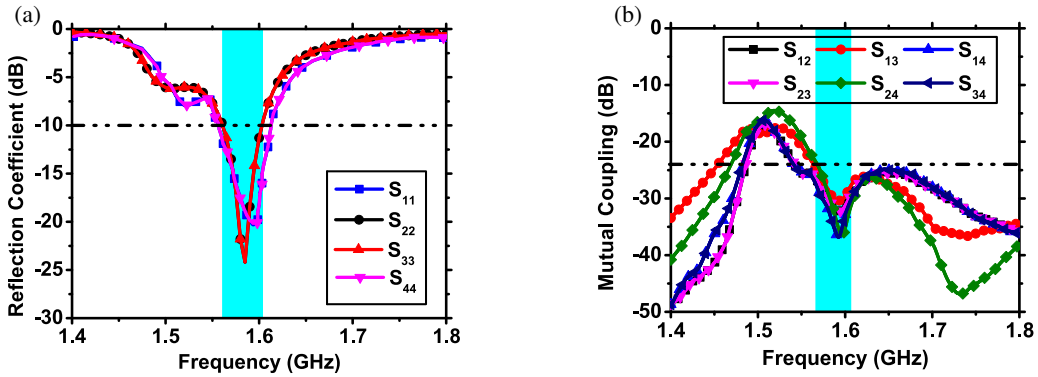

FIGURE 15. Simulation results of the proposed array with DGS and meta-isolator. (a) Reflection coefficient. (b) Mutual coupling.

TABLE 1. Comparison of presented design with existing literature.

Reference #	[5]	[7]	[8]	[14]	[15]	[16]	[17]	[18]	**Proposed**
Area (cm^2)	119.29	122.65	122.65	153.20	400	361	196	184.96	**122.65**
No. of Elements	4	4	4	3	5	4	4	4	**4**
GNSS bands Covered	L1, L2	L1, B1, E1, G1	B1, L1, E1, G1	L1	B1, L1	B3	B3	B1, L1, E1, G1	L1, B1, E1, G1
Isolation (dB)	$>$ 15, 25	$>$ 20	$>$ 25	$>$ 18.6	$>$ 20	$>$ 22	$>$ 18	$>$ 20	$\mathbf{> 24}$
Gain (dBi)	-	$>$ 3.3	$>$ 5.75	-	$>$ 4	-	-	$>$ 6	$\mathbf{> 6.9}$
Efficiency	-	$>$ 38%	$>$ 58.8%	-	-	-	$>$ 52%	-	$\mathbf{> 93\%}$

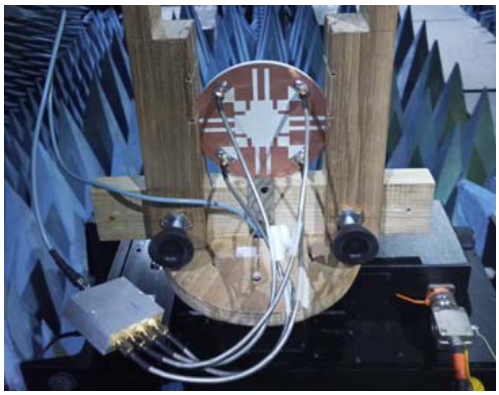

FIGURE 16. DGS and meta-isolator array placed in anechoic chamber for radiation pattern measurement.

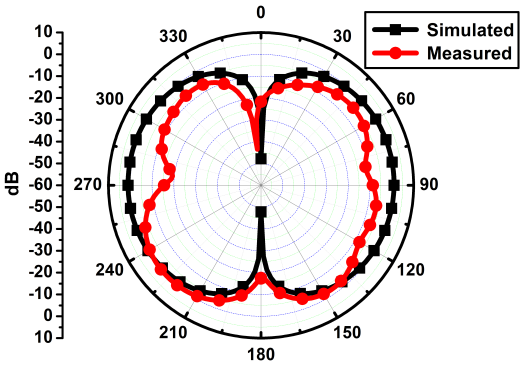

FIGURE 17. Measured and simulated radiation pattern of the fabricated model with a null formed.

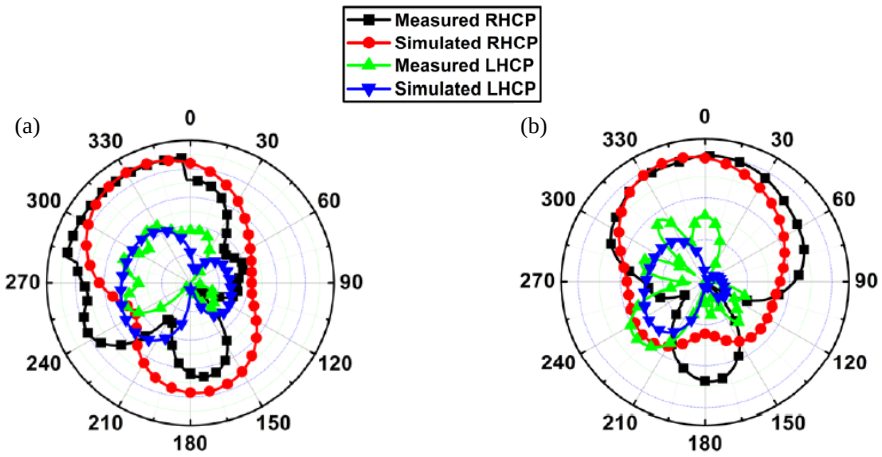

FIGURE 18. (a) Simulated and measured normalized RHCP and LHCP patterns for E-plane. (b) Simulated and measured normalized RHCP and LHCP patterns for H-plane.

The proposed antenna is compared with previously published works on the basis of size, number of GNSS bands covered, isolation level, gain, and efficiency. The size of the presented antenna is significantly less than the designs reported in [14–18]. The proposed antenna also covers more GNSS bands than [5, 14–17] making it more robust and versatile. The isolation level of the proposed design is also more than described in [7, 14–18]. Furthermore, the gain and efficiency of our proposed design are significantly greater than the previous designs [7, 8] employing an absorber that degrades these two essential parameters. The design complexity of the proposed design is also significantly less than [5, 16] which employ a vertical wall of split ring resonators (SRRs), increasing the vertical height of the antenna arrays. Hence, the presented four-element antenna array surpasses the earlier published GNSS arrays due to more GNSS bands covered, compact size, higher isolation level, higher gain, more efficiency, and design simplicity.

6. CONCLUSION

In this manuscript, we introduce a compact four-element high-isolation antenna array designed for applications in the GNSS upper L-band. The proposed design achieves compactness by using a high epsilon substrate while simultaneously retaining an isolation of more than 24 dB by employing a DGS and novel meta-isolator. The proposed antenna covers all the GNSS bands of interest in the upper L-band, i.e., GPS L1 (1.575 GHz), BeiDou B1 (1.561 GHz), Galileo E1 (1.575 GHz), and GLONASS G1 (1.602 GHz). The proposed design exhibits excellent RHCP realized gain indicating suitable polarization purity. The radiation efficiency of the presented design is more than 93% while the gain is more than 6.9 dBi. Owing to its compact size, high isolation, and high efficiency, the proposed design is an ideal option for robust GNSS multi-band applications. In future works, the proposed research can be extended by exploring more techniques to achieve further miniaturization and compactness while simultaneously maintaining a better isolation level. Additionally, enhancing the array's gain can be pursued by increasing the number of array elements.

REFERENCES

[1] Sanz Subirana, J., J. M. J. Zornoza, and M. Hernández-Pajares, "GNSS signal," Technical University of Catalonia, 2011.

[2] Molisch, A. F. and M. Z. Win, "MIMO systems with antenna selection," *IEEE Microwave Magazine*, Vol. 5, No. 1, 46–56, Mar. 2004.

[3] Hui, H. T., "Reducing the mutual coupling effect in adaptive nulling using a re-defined mutual impedance," *IEEE Microwave and Wireless Components Letters*, Vol. 12, No. 5, 178–180, May 2002.

[4] Yang, F. and Y. Rahmat-Samii, "Microstrip antennas integrated with electromagnetic band-gap (EBG) structures: A low mutual coupling design for array applications," *IEEE Transactions on Antennas and Propagation*, Vol. 51, No. 10, 2936–2946, Oct. 2003.

[5] Gheethan, A. A., P. A. Herzig, and G. Mumcu, "Compact 2 x 2 coupled double loop GPS antenna array loaded with broadside coupled split ring resonators," *IEEE Transactions on Antennas and Propagation*, Vol. 61, No. 6, 3000–3008, Jun. 2013.

[6] Gheethan, A. and G. Mumcu, "Coupling reduction of coupled double loop gps antennas using split ring resonators," in *2011 IEEE International Symposium on Antennas and Propagation (APSURSI)*, 2613–2616, IEEE, Spokane, WA, Jul. 2011.

[7] Awais, M., A. Madni, and W. T. Khan, "Design of a compact high isolation 4-element wideband patch antenna array for GNSS applications," *IEEE Access*, Vol. 10, 13 780–13 786, 2022.

[8] Madni, A. and W. T. Khan, "Design of a compact 4-element GNSS antenna array with high isolation using a defected ground structure (DGS) and a microwave absorber," *IEEE Open Journal of Antennas and Propagation*, Vol. 4, 779–791, 2023.

[9] Tamjid, F., F. Foroughian, C. M. Thomas, A. Ghahreamani, R. Kazemi, and A. E. Fathy, "Toward high-performance wideband gnss antennas-design tradeoffs and development of wideband feed network structure," *IEEE Transactions on Antennas and Propagation*, Vol. 68, No. 8, 5796–5806, 2020.

[10] Chen, X., C. G. Parini, B. Collins, Y. Yao, and M. U. Rehman, *Antennas for Global Navigation Satellite Systems*, John Wiley & Sons, 2012.

[11] Huang, J., "A technique for an array to generate circular polarization with linearly polarized elements," *IEEE Transactions on Antennas and Propagation*, Vol. 34, No. 9, 1113–1124, 1986.

[12] Kovitz, J. M. and Y. Rahmat-Samii, "Using thick substrates and capacitive probe compensation to enhance the bandwidth of traditional CP patch antennas," *IEEE Transactions on Antennas and Propagation*, Vol. 62, No. 10, 4970–4979, 2014.

[13] Narbudowicz, A. Z., "Advanced circularly polarised microstrip patch antennas," Ph.D. dissertation, Technological University Dublin, 2013.

[14] Byun, G., H. Choo, and S. Kim, "Design of a small arc-shaped antenna array with high isolation for applications of controlled reception pattern antennas," *IEEE Transactions on Antennas and Propagation*, Vol. 64, No. 4, 1542–1546, Apr. 2016.

[15] Liu, Y., S. Zhang, and Y. Gao, "A high-temperature stable antenna array for the satellite navigation system," *IEEE Antennas and Wireless Propagation Letters*, Vol. 16, 1397–1400, 2016.

[16] Zhang, J., J. Li, and J. Chen, "Mutual coupling reduction of a circularly polarized four-element antenna array using metamaterial absorber for unmanned vehicles," *IEEE Access*, Vol. 7, 57 469–57 475, 2019.

[17] Li, J., H. Shi, J. Guo, and A. Zhang, "Compact four-element antenna array design for BeiDou Navigation Satellite System applications," *Progress In Electromagnetics Research Letters*, Vol. 57, 117–123, 2015.

[18] Wei, J., S. Liao, Q. Xue, and W. Che, "Highly integrated multifunctional antenna for Global Navigation Satellite System," *IEEE Transactions on Antennas and Propagation*, Vol. 70, No. 12, 12 305–12 310, 2022.